GIP test for Automotive FMCW interference Detection and Suppression

Thomas Pernstål, Johan Degerman, Henric Broström, Viet Thuy Vu, *Member, IEEE,* Mats I. Pettersson *Member, IEEE,*

***Abstract*—This paper addresses the problem of mutual interference between automotive radars. The rapid growth of automotive and commercial radar systems on the market does not only facilitate new applications, e.g., advanced driver assistant systems, but also put demands on the possibilities for co-existence, i.e. cohabitant systems. For military radar systems, various jammer and interference mitigation methods have been extensively analyzed and evaluated for decades. However, until now, the co-existence and influence of jamming/interference have almost been ignored for the commercial radar business. A Generalized Inner Product, GIP, test based outlier detector and interference estimation is presented here, which suppress the interferences only in those Directions of Arrival, DOA, and time domain portions where the nuisance signals appear. We will denote this GIP test based Interference Detector and Suppression as the GIDS method. Using GIDS, the target detection performance for the specific interference DOA will merely have a small loss instead of being completely suppressed, e.g., sample matrix inversion implementation of spatial nulling. The proposed technique is robust and does not rely on any calibration for the interference cancellation. Based on simulation and experimental data, we have shown that without losing target detection performance, we achieved up to about 30 dB enhancement for the Signal to Interference and Noise Ratio.**

***Index Terms*—mm-wave FMCW radar, interference mitigation, GIP outlier detection**

I. Introduction

The rapid growth of automotive radar system on the market not only facilitates new applications like sophisticated Advanced Driver Assistant Systems (ADAS) functions, e.g. rear cross traffic alert, and intersection Automatic Emergency Braking (AEB), autonomous parking, simultaneous localization and mapping (SLAM), freespace grid, and so on, but also makes the signal environment very challenging since all radar systems are located in the same frequency band employing simple frequency chirp waveforms. This could be compared with the situation for the mobile communication systems for about 30 years ago.

From the MOSARIM analysis, [1], conducted 7 years ago it was strangely concluded that interference from different radar systems could almost be neglected in terms of performance loss. This analysis was merely considering slow chirp and low bandwidth FMCW waveforms and thus this might be one of the reasons for this more or less misleading conclusion.

Moreover, the theoretical foundation of multi-channel sensor array systems, that provides the ability to extract or reject signals, is called array signal processing. Here, one applies detection and estimation theory, which in radar theory have always been employed for temporal characteristics of the signal, to the entire problem of discriminating signals in time and space. We refer to [2], [3] for an overview of this research. While array signal processing is a general theory not specific to any type of sensor, it has successfully been applied to the radar application. The literature is extensive, see e.g [4], [5], [6], [7], [8], and references therein. Utilizing Multi-Channel sensor Arrays (MCA), several interferer signals can be suppressed. More specifically,a MCA that consists of N channels provides the possibility to suppress N-1 narrow band jammer signals [3]. By narrow band we mean a signal that covers less than one percent bandwidth, e.g., 100 MHz at X-band. Now, in common arraysignal processing algorithms, e.g. the Sample Matrix Inversion (SMI) detector [9], the estimation of the covariance matrix and the weight vector adaptation is made using data samples known as secondary data. The secondary data is assumed to be signal free and statistically independent of the data to which the weight vector is applied, i.e., the primary data. Clearly, the essence in jammer suppression is to access secondary data which provides a confident estimate of the interference covariance matrix. In other words, the ability to suppress N-1 narrow jammer signals degrades if the spatial covariance estimate deviates from the true directions of the jammer signals.

In most of the published literature regarding array signal processing, only non-fluctuating/non-adaptive jammer/interference scenarios are analyzed. In other words, in the case of jammer signals with time varying properties, the literature is scarce. There are however some interesting papers that discuss and analyze the jammer/interference rejection ability of an MCA system when it is subjected to jammer signals with different polarization states [1], [2]. In [1], a feasible approach of investigating the influence of polarization agile jammers is presented. This approach is based on representing the change of the polarization state by a complex excitation error that is imposed on the true steering vector. Moreover, in [10] a novel approach for adaptive interference cancellation adopted for automotive radar is shown. This approach relies on the time domain data employing spatial suppression by adapting a filter (weights) based on the time domain data. In this paper it is shown that the results are very promising.

Thomas Pernstål, Johan Degerman, Henric Broström, are with SafeRadar Research Sweden AB, 431 35 Mölndal, Sweden. E-mail: thomas.pernstal@saferadar.se,johan.degerman@saferadar.se,Henric Broström@saferadar.se.

V. T. Vu, M. I. Pettersson are with Blekinge Institute of Technology, 37179 Karlskrona, Sweden. E-mail: viet.thuy.vu@bth.se, mats.pettersson@bth.se.

Manuscript received February 26, revised May 9, accepted June 24 2018.

However, the interference identification framework is simple where the outliers are based on non-sinusoidal behavior of the received signals. Thus, in a dense environment where many targets and interferers are present it is typically difficult to adapt such a framework to a desired false alarm rate.

In this paper we instead employ well know frameworks for outlier screeningin order to mitigate the influence of interference. The origin of this idea comes from the heterogeneous clutter screening where one can employ non-homogeneity detection (NHD) or design detectors that in some way are robust to heterogeneity [11], and [12]. For the heterogeneous clutter case, the idea of this NHD is to detect which of the training data range bins that are not homogeneous, and then remove them from the estimation of the covariance matrix. For the FMCW interfering case we want to adopt the same approach but here we instead are screening the baseband signal (after mixing with the received RF signal) in order to detect the DOAs of interferers (or outliers).

In this paper the NHD analysis is given by the generalized covariance based Generalized Inner Product (GIP) statistics, [5] [6], [13], and [14]. The resulting performances using this outlier detection approach is then compared with the simple and commonly used Post Doppler based Sample Matrix Inversion (SMI) method in terms of suppression capability and sensitivity loss.

II. FMCW/FCM Interference problem and SMI suppression

In [10], [15] and also in [1], the influence of the FMCW waveform emitter interference impact discussed and analyzed. In Figure 1 we illustrate this issue where also the typically used Fast Chirp Modulation, FCM, waveform is shown. From Figures we also observe that the interference is intermittent since this intersection between the interfering and real signal moves through the chirp train, assuming different chirp rates.

After dechirping, i.e., mixing the in and out signals, the received and interfering signal to baseband we typically obtain an Range Doppler outcome, i.e., after making the range-Doppler Processing based on a 2D FFT, as shown in Figure 1. Note that the host (or EGO) vehicle, being subjected to interference, is moving at a speed of 2 m/s. The interfering system was using a chirp duration of 40 μs and 500 MHz chirp bandwidth. The system subjected to interference was using a chirp duration of 40 μs and 1 GHz chirp bandwidth.

To mitigate the influence of interference, a commonly employed method is adaptive spatial nulling relying on the Sample Matrix Inversion (SMI) Method

More specifically, the suppression weights of the Sample Matrix Inversion (SMI) method are computed as follows [3], and [2]

$$\mathbf{w} = \mathbf{R}^{-1}\mathbf{s} \approx \hat{\mathbf{R}}^{-1}\mathbf{s} \tag{1}$$

where $\mathbf{s}$ is the (spatial) steering vector and the estimated (spatial) sample covariance matrix, $\hat{\mathbf{R}}$, is given by

$$\hat{\mathbf{R}} = \frac{1}{N}\sum_{k=1}^{N}\mathbf{v}_k\mathbf{v}_k^h \tag{2}$$

where $\mathbf{v}_k$ is the acquired post-Doppler processed data of all channels at training bin k. The covariance matrix, $\hat{\mathbf{R}}$, becomes a N_{ch} by N_{ch} space-matrix where N_{ch} is the number of receiving channels, i.e., the number of spatial channels.

To determine if interference is present we need to introduce a threshold that tells us if we have interference or not. This could typically rely on the estimated power of the interference. That is

$$trace\left(\hat{\mathbf{R}}\right) > \eta_{jam} \tag{3}$$

where $trace$ denotes the diagonal sum (i.e., the sum of the diagonal elements) and η_{jam} is the threshold of interference power level deciding if interference is present or not.

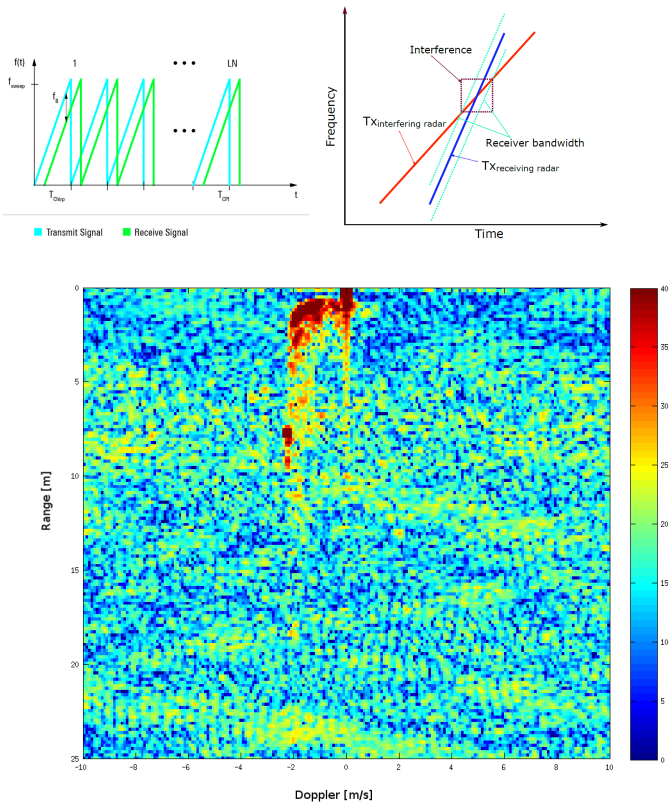

Fig. 1. Upper Left insert illustrates the conventional Fast Chirp FMCW waveform (FCM) and the upper right insert shows when a FCM/FMCW radar is subjected to FCM/FMCW interference. Courtesy [10]. The lower insert illustration of when a FMCW radar is subjected to FMCW interference (measurement data at 77 GHz). Note that the x-axis and y-axis show the Doppler and Range, respectively. The radar subjected to interference is the so called "Vinnova"-radar developed in a Swedish Research Program. Note that 0 dB corresponds to the noise level of the systems and the "yellow" stripes along Doppler is due to the interference.

III. GIP based Interference Detection and Suppression (GIDS)

In this section we describe the GIP based Pre-Range and Pre-Doppler outlier scanning.

One way of measuring homogeneity of the signal contents is the so called "generalized inner product" (GIP) statistic. Assume we have a data matrix of N channels and K bins.

$$\mathbf{X} = \begin{pmatrix} x_{11} & x_{12} & \cdots & x_{1n} & \cdots & x_{1N} \\ x_{21} & x_{22} & \cdots & x_{2n} & \cdots & x_{2N} \\ \vdots & \vdots & \ddots & \vdots & \ddots & \vdots \\ x_{k1} & x_{k2} & \cdots & x_{kn} & \cdots & x_{kN} \\ \vdots & \vdots & \ddots & \vdots & \ddots & \vdots \\ x_{K1} & x_{K1} & \cdots & x_{Kn} & \cdots & x_{KN} \end{pmatrix} = \begin{pmatrix} \mathbf{x}_1 \\ \mathbf{x}_2 \\ \vdots \\ \mathbf{x}_k \\ \vdots \\ \mathbf{x}_N \end{pmatrix} \tag{4}$$

Now, let $\mathbf{x} = [\mathbf{x}_1, \mathbf{x}_2, \ldots, \mathbf{x}_N]$ denotes a complex random vector that is distributed as complex Gaussian with zero mean and known positive Hermitian covariance matrix,$\mathbf{R}$, i.e., $\mathbf{x} \sim CN(0, \mathbf{R})$. Then the quadratic form $Q = \mathbf{x}^H \mathbf{R}^{-1} \mathbf{x}$ has mean $E(Q) = N$ and is chi-square distributed [16]. Now if we use the sample covariance matrix estimate, $\hat{\mathbf{R}}_k$, based on our training data we get the GIP statistic

$$P_k = \mathbf{x}_k^H \hat{\mathbf{R}}_k^{-1} \mathbf{x}_k \qquad \hat{\mathbf{R}}_k = \frac{1}{K} \sum_{l \neq k} \mathbf{x}_l \mathbf{x}_l^H \tag{5}$$

Moreover, it is shown in [16] that P_k can be seen as the ratio between two independent chi-square distributed random variables (i.e. it follows a F-distribution), and that $\lim_{K \to \infty} E(P_k) = N$. Note that the covariance matrix, $\mathbf{R}$, will be a spatial covariance given by the receiver channels of the radar antenna array.

Loosely speaking, the GIP approach means that we try to sort out training samples that deviate too much from the estimated covariance. Typically, screening based on GIP statistics sort out samples either based on using a threshold or a fix number of samples, e.g., 25 percent are removed and 75 percent are kept for covariance estimation. Note that the threshold method needs to ensure that the remaining number of training samples is sufficient when estimating the covariance.

The GIP statistic was introduced in [5] by Melvin et. al. as a non-homogeneity detector, and have since been used in various situations. In [5], range bins for which the P_k values deviated to much from the mean of all P_k were discarded from the covariance matrix estimation used for the STAP. There is a problem in using the GIP statistic in heterogeneous data since a test using P_k assumes homogeneous data are used to form $\hat{\mathbf{R}}_k$. A iterative (multi-pass) method, that after censoring a number of range bins makes a new covariance matrix estimate and computes a new GIP statistic based on that, can reduce this problem [6], [13].

In this paper we employ the GIP approach prior to the range and Doppler processing, i.e., so called baseband signal. This means that the pre-Doppler (spatial) covariance matrix, $\hat{\mathbf{R}}_{\mathbf{Pre}}$, for one downconverted single chirp (baseband) in the chirp train received is given by

$$\hat{\mathbf{R}}_{\mathbf{Pre}} = \frac{1}{N-1} \sum_{k=1}^{N} \mathbf{x}_k \mathbf{x}_k^h \tag{6}$$

where $\mathbf{x}_k$ is the acquired baseband sample data for that single de-chirp signal, i.e., prior range and Doppler processing. The data, $\mathbf{x}_k$, is a vector of a length equal to all receiving spatial channels at the baseband (after AD-converter) sample bin k (or time k).

To make the interference suppression we examine the outcome from the GIP statistics. Assume we have a pre-defined threshold, η_{gip}, the we select the GIP samples exceeding this threshold. That is

$$P_k = \mathbf{x}_k^H \hat{\mathbf{R}}_{\mathbf{Pre}_k}^{-1} \mathbf{x}_k \quad > \quad \eta_{gip} \tag{7}$$

Now, we denote these outlier samples as $\mathbf{x}_{out}$. Note that the inlier samples are denoted as $\mathbf{x}_{in}$. That is

$$\mathbf{x} = \begin{cases} \mathbf{x_{in}} & \mathbf{x}^H \hat{\mathbf{R}}_{\mathbf{pre}}^{-1} \mathbf{x} < \eta_{\text{gip}} \\ \mathbf{x_{out}} & \mathbf{x}^H \hat{\mathbf{R}}_{\mathbf{pre}}^{-1} \mathbf{x} \geq \eta_{\text{gip}} \end{cases} \tag{8}$$

Here it is noteworthy that the pre-defined threshold, η_{gip}, is computed based on the desired false alarm rate achieved from the GIP statistics, see Equation 5.

To compute the interference covariance we first need to remove the targets signals in the baseband signal before we estimate the interference directions. To remove the target signals, we pre-white the samples by using, $\hat{\mathbf{R}}_{\mathbf{Pre}}$, by computing

$$\mathbf{z}_{out} = \mathbf{x}_{out} \hat{\mathbf{C}}^{-1} \tag{9}$$

where we employ Cholesky decomposition to find $\hat{\mathbf{R}}_{\mathbf{Pre}} = \hat{\mathbf{C}} \hat{\mathbf{C}}^H$.

Next, we compute the (spatial) covariance matrix, $\hat{\mathbf{R}}_{out}$, originating from the interferences as follows (skipping the pre-Doppler notation)

$$\hat{\mathbf{R}}_{out} = \frac{1}{M-1} \sum_{m=1}^{M \leq N} \mathbf{z}_{out} \mathbf{z}_{out}^H \tag{10}$$

Where M is the number of GIP samples, i.e., outliers, detected.

The weighting vectors are computed as for the SMI approach [17]. That is

$$\mathbf{w} = \hat{\mathbf{R}}_{out}^{-1} \mathbf{s} \tag{11}$$

Here it is noteworthy that for this pre-whitening step [3], we have a fundamental restriction: the covariance matrix for the noise must have full rank and be positive semidefinite. This is crucial since the pre-whitening step essentially consists of multiplying the signal matrix with the inverse of the Cholesky factor of the noise covariance matrix.

Finally, we can impose the interference suppression in two different ways. For the first and simplest approach we merely use the computed weight vector when making the beamforming process, i.e., steering the beams digitally in order to scan and detect targets . That is

$$\mathbf{y} = \begin{cases} \mathbf{y_{in}} = \mathbf{s^H x} & \mathbf{x} < \eta_{\text{GIP}} \\ \mathbf{y_{out}} = \mathbf{w^H x} & \mathbf{x} \geq \eta_{\text{GIP}} \end{cases} \tag{12}$$

where $\mathbf{y}$ is the coherently summed beams using all receiver channels. Note that these coherent beams are computed for all directions, steering vectors, of interest.

The other and more sophisticated way to mitigate this interference is to facilitate the ability to still employ a multi-channel detection and estimation framework after this interference mitigation. That is, instead of computing the coherent beam $\mathbf{y}$, we pre-white the received data $\mathbf{x}$. In other words, we suppress the detected interference samples for each spatial receiver channel using the Cholesky decomposed version of the estimated interference covariance $\hat{\mathbf{R}}_{out}$. , that is

$$\tilde{\mathbf{x}}_{\mathbf{out}} = \mathbf{x}_{\mathbf{out}} \hat{\mathbf{C}}_{\mathbf{out}}^{-1} \tag{13}$$

where $\hat{\mathbf{R}}_{out} = \hat{\mathbf{C}}_{out} \hat{\mathbf{C}}_{out}^{H}$. Now the received radar samples (pre-Doppler) provided to the detection and estimation framework becomes

$$\tilde{\mathbf{x}} = \begin{cases} \mathbf{x}_{\mathbf{in}} & \mathbf{x}^H \hat{\mathbf{R}}_{\mathbf{pre}}^{-1} \mathbf{x} < \eta_{\text{gip}} \\ \tilde{\mathbf{x}}_{\mathbf{out}} & \mathbf{x}^H \hat{\mathbf{R}}_{\mathbf{pre}}^{-1} \mathbf{x} \geq \eta_{\text{gip}} \end{cases} \tag{14}$$

where x_{in} and $\tilde{x}_{out}$ corresponds to the inlier and outlier samples based on the GIP test, respectively. In Figure 2 we show the flowchart of the operations made in GIDS.

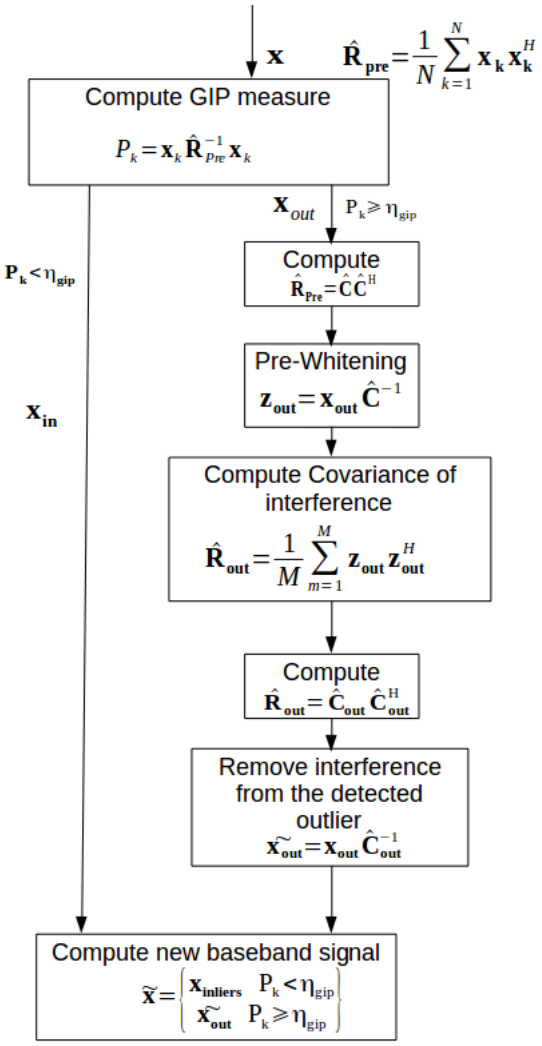

Fig. 2. Flowchart of the GIDS framework GIP statistics, respectively.

IV. Simulations

To simulate this we have employed a simple multi-channel aperture based on eight channel receiver layout in an ULA configuration, i.e., the phase centers are separated by half a wavelength along the horizontal axis.

The setups of the simulation are as follows. In case 1 we use a single point target at a range of 10 m having an SNR of 30 dB. The target velocity is 10 m/s where the target is located at boresight. The host radar bandwidth is 1 GHz using a chirp duration of $40\mu s$. The interferer is located at a DOA of 20 degrees in azimuth using a bandwidth 2 GHz using a chirp duration of $40\mu s$. The Jammer to Noise Ratio (JNR) of interferer is 30 dB.

In case 2 we have increased the complexity of scenario where it consist of two targets and two interfererers. The target ranges are 10 m and 20 m where both targets have a speed of 10 m/s. The DOAs of of the targets are given at boresight and 20 degrees in azimuth (horizontally). The interferences are given for azimuth angles at 10 and 20 degrees, respectively. Thus, the DOAs for one of the targets and one of the interferers are given at the same azimuth angle, i.e., 20 degrees along azimuth. The host radar bandwidth is 1 GHz using a chirp duration of $40\mu s$. The interferers employes a chirp bandwidth of 1.5 GHz and 2 GHz, respectively, where both the interferes are using a chirp duration of $40\mu s$.

Scenario	Case 1	Case 2	**Unit**
Number of targets	1	2	[-]
Number of interferers	1	2	[-]
Target Range/ Velocity	10 / 10	10, 20 / 10,10	[m] and [m/s]
Target DOA Azimuth	Boresight	Boresight , 20 degrees in azimuth	[deg]
SNR	30	30, 20	[dB]
Hosts/EGO Radar Bandwidth	1	1	[GHz]
Interference Bandwidth	1	1.5, 2	[GHz]
Interference DOA (Azimuth)	20	10, 20	[deg]
JNR	30	30, 30	[dB]

TABLE I
SUMMARY OF SIMULATED TEST CASES ANALYZED

In Figure 3 we show the baseband signal (pre-Doppler and range) outcome and the GIP statistics for the case 1 scenario. From the figure we clearly can obseve the peak indicating the interference.

Next step is to find a proper threshold based on the test statistics. In [16], they have derived that the GIP statistics follows the Student-t distribution. Using this, and simulated 500,000 complex-Gaussian samples aiming for a probability of false alarm of 10^{-5} . This yielded a normalized GIP threshold, i.e., normalized by the number of samples, N used, η_{gip}, of 0.05.

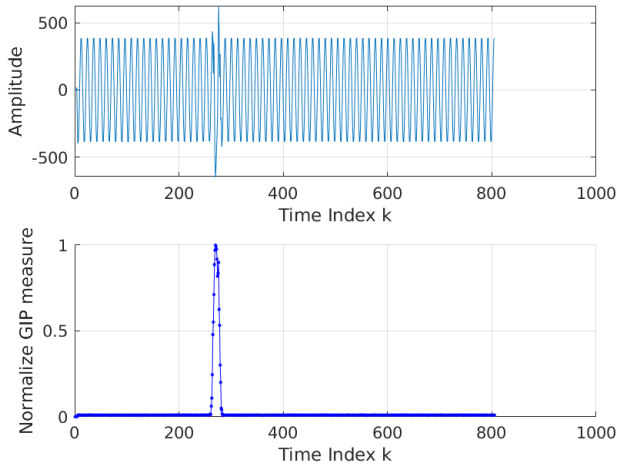

Fig. 3. The upper and lower sub plots show the baseband signal in present of interference for case 1 and the corresponding GIP statistics, respectively. Note that each time index corresponds to a baseband sample rate of 20 MHz

Thereafter, we want to examine the behavior using this threshold and make the suppression based on the covariance estimated for those samples that are indicated as interfered (by the GIP measure). In other words, for those samples labeled as interfered we employ simple SMI based suppression. Please note that, to avoid matrices close to singular, i.e., large condition number, we employ diagonal loading, i.e.,

$$\hat{\mathbf{R}} = \beta \mathbf{I}_N + \frac{1}{K} \sum_{k=1}^{K} \mathbf{x}_k \mathbf{x}_k^H \tag{15}$$

where k indicate the samples that are interfered. Please note that on [18] the use of diagonal loading to overcome low sample size for adaptive beamforming is described thoroughly. Other interesting papers are [19], and [20]. Typical values of β is 10-100, i.e., 10-20 dB above noise floor. In this paper, we have used a β value of 10. The corrected baseband signal outcome using this suppression is shown in Figure 4. From the Figure, we can clearly observe that the interfering signal is removed

To understand this GIP measure based method we show the MUSIC spectra's extracted for different parts of the chirp regarding the case 1 scenario. In Figure 4, we show the MUSIC spectra's using the eight channel ULA antenna configuration. From the Figures, we clearly can observe that the interference yield an additional signal DOAs. Thus, using a spatial covariance of the GIP measure that is estimated using the entire chirp, i.e., the outcome in the top insert, we can clearly see that it is easy to detect this "spatial" outlier when the interference is present (the bottom insert).

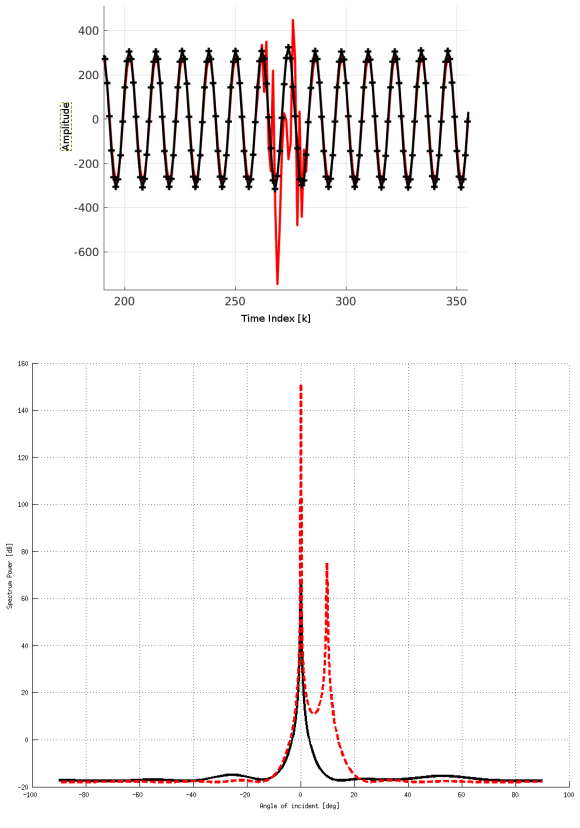

Fig. 4. Upper insert show the baseband sampling outcome prior to (red solid) and after mitigation of the interference (black solid with cross). The x and y axis represent the baseband samples (time index k) and signal amplitude, respectively. The lower insert show the MUSIC spectrum outcome using data over the part of data where only the signal is present (black solid) and where both signal and interference is present (red dashed).

Next, we want to examine this for the case 2 scenario that also emphasize the target detection performance before and after the interference suppression has been made. At first, we show and examine the range Doppler outcome without interference suppression. In Figure 5 we observe that the Signal to Noise Ratio for both of the targets are at the same level as the the interferer level, i.e., JNR. Thus we can almost distinguish the target points in the range Doppler outcome. We compute the normalize GIP measure in Figure 5. From the Figure, we can clearly observe the interfering signals in the GIP measure. In Figure 5 we also show the baseband signal before and after suppression. Using the corrected baseband signal outcome shown in Figure 5 and make range and Doppler processing we achieve a result that is shown in Figure 5. From the Figure, we can clearly observe that the interfering signal is suppressed (almost removed). The Signal to Interference and Noise ratio (SINR) has been improved by about 30-40 dB, see Figure 5.

Finally, we will compare this method with a regular post Doppler SMI suppressing method, see section II. In Figure 6 we can clearly observe that the GIDS method outperforms the post Doppler SMI spatial nulling method since the second target is completely suppressed by this method (having the same direction as the interferer). In addition to this, the

interferences are not completely removed due to poor estimates of the spatial covariances in presence of the targets.

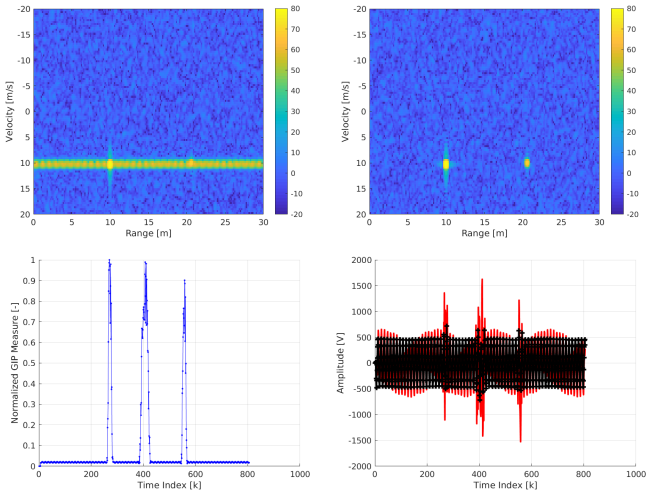

Fig. 5. Upper left and right inserts show the range-Doppler without suppression and using this interference suppression for all chirps, respectively. Lower insert show the GIP and baseband outcome, prior and after suppression. Note that in this case the two interfering signals crosses the receiving chirp three times due to different chirp rates and thus we get three peaks.

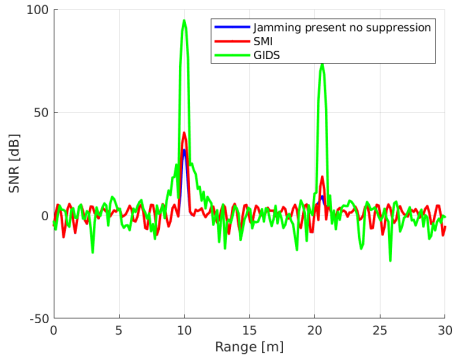

Fig. 6. Shows the improvement of using GIDS versus SMI where the interference level/noise level is normalized to 0 dB. Thus this presents the Signal to Interference ratio measure

V. Analysis using Experimental Data

In this section we analyze this Pre-Doppler interference mitigation technique using experimental data collected in an anechoic chamber, see Figure 7. In this Figure we also show the evaluation board from TI (1243) used to collect the interfered radar data. In Figure 7 we show the outcome when one of 77 GHz radar system is subjected one 1 GHz interference. The system itself, i.e., the receiving and analyzed system, employs 500 MHz bandwidth using the same chirp duration ($40\mu s$). As reference targets, the test case comprises a corner reflector at boresight and at a range of 4 m for the radar systems.

To examine the behavior of this method we use one of the outcomes that seems to be a fairly weak interference case. In the Figure 7 we show the incoherently summed Range Doppler outcomes having the interference present. The JNR of interference is estimated to about 15 dB. Please note that since the host radar is not moving, both static objects, DC-noise and interferers are located in the same Doppler channel, i.e., zero Doppler. Thus, since it is difficult to observe improvements after interference suppression, we will only examine influence for the baseband signal prior to and after interference mitigation. Moreover, to we analyze the pre-Doppler outcome from one of the chirps and employ the GIP measure onto the baseband signal in order to assess where in time of each chirp we have this interference. In Figure 7 we show the Pre-Doppler outcome, i.e., the coherent sum channel at boresight, with the interference present and GIP statistics from these measurements. In Figure 7 , we show the outcome when using the GIDS method. To reduce the false alarm rate for the GIP detector, we have added a margin of 10 % compared to the theoretically computed GIP thresholds. The reason for this might be that the data samples are not complex Gaussian distributed. From the Figure, we observe that signal to interference ratio (SINR) has increased and that the interference is suppressed. Note that the sum beam direction is the boresight direction, i.e., the position for the corner reflector.

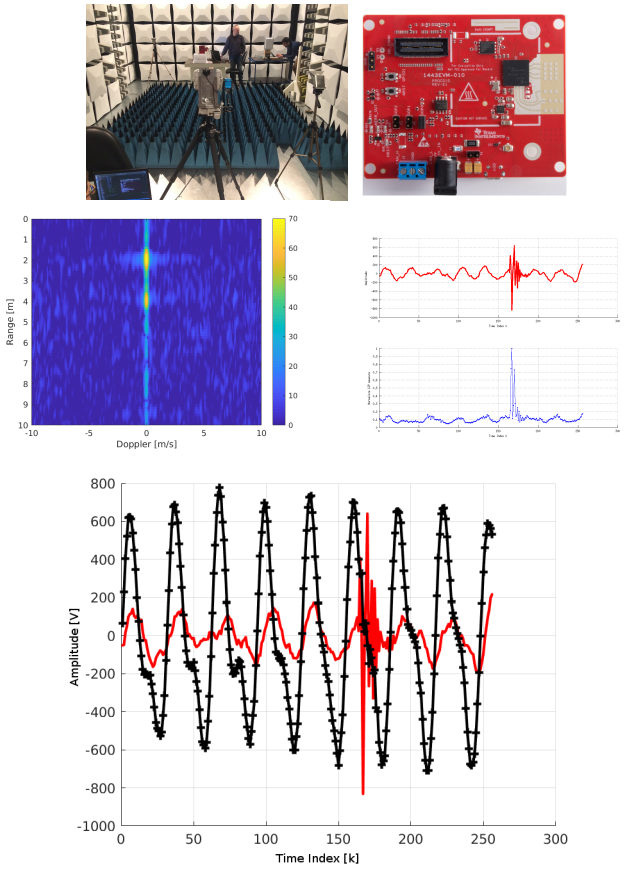

Fig. 7. Photo of the anechoic chamber setup and the radar subjected to interference. Lower left insert show the Incoherently summed Range Doppler outcomes having the interference present. The interference and the radar subjected to the interference employs 1 GHz bandwidth and 500 MHZ, respectively. The lower center insert shows the baseband chirp outcome (real part) and the GIP measure with interference present, respectively. The lower right insert shows the baseband sampling outcome prior to (red solid) and after mitigation of the interference (black solid with cross) using GIDS suppression.

VI. Conclusions and Future work

In this paper we have described a novel method used for mitigating the influence of automotive radar interference. The method is denoted as GIDS and utilizes an interference detection framework based on DOA anomalies of the baseband signal. The simulation results and the comparison using experimental data show that the algorithm is powerful, particularly for weak interferences that typically are difficult to detect. More specifically, the GIDS framework is compared with the conventional SMI framework where it is shown, in particularly for weak interferences levels, that the sensitivity of the GIDS framework outperforms the SMI version. Thus from this we can infer that the GIDS framework used for interference suppression has a great capability and potential.

In this paper we have only been using the GIP measure to detect DOA anomalies. However, in the literature a vast number of measures can be used for this where one of the most interesting in a DOA perspective is given in paper [21].

The future work also comprises deriving a framework that also fully reconstruct the baseband signal where the interference is present, see [10]. In other words, this result in a milder suppression of the targets located in the same direction as the interferer. Thus, this will enhance the GIDS framework even further.

References

[1] Mosarim, "More safety for all by radar interference mitigation (mosarim)," Tech. Rep., European collaboration (EU funding), Germany, 2010.

[2] Richard Klemm, *Principles of space-time adaptive processing*, The Instiution of Electrical Engineers, 2002.

[3] Harry L. Van Trees, "Optimum array processing. part iv of detection, estimation and modulation theory," Tech. Rep., John Wiley and Sons Inc., New York, 2002.

[4] Mats Viberg and Björn Ottersten, "Sensor array processing based on subspace fitting," *IEEE Transactions on Signal Processing*, vol. 39, no. 5, pp. 110–1121, may 1991.

[5] William L. Melvin, Michael C. Wicks, and Russell D. Brown, "Assessment of multichannel airborne radar measurements for analysis and design of space-time processing architectures and algorithms," in *Proceedings of the 1996 IEEE National Radar Conference*, 1996, pp. 130–135.

[6] William L. Melvin and Michael C. Wicks, "Improving practical space-time adaptive radar," in *Proceedings of the 1997 IEEE National Radar Conference*, 1997, pp. 48–53.

[7] Richard Klemm, "STAP for circular forward looking array antennas," in *Radar 97 conference*, 1997, pp. 300–304.

[8] Joseph R. Guerci and Edward J. Baranoski, "Knowledge-aided adaptive radar at DARPA," *IEEE Signal Processing Magazine*, vol. 23, no. 1, pp. 41–50, jan 2006.

[9] T.K. Truong I.S. Reed, Y.L. Gau, "Cfar detection and estimation for stap radar," in *IEEE Transactions on Aerospace and Electronic Systems*, 1998.

[10] Mats I. Pettersson Muhammad Rameez, Mattias Dahl, "Adaptive digital beamforming for interference suppression in automotive fmcw radars," in *Radar Conference, IEEE*, 2018.

[11] William L. Melvin, "Space-time adaptive radar performance in heterogeneous clutter," *IEEE Transactions on Aerospace and Electronic Systems*, vol. 36, no. 2, pp. 621–633, apr 2000.

[12] William L. Melvin, "A STAP overview," *IEEE Aerospace and Electronic Systems Magazine*, vol. 19, no. 1, pp. 19–35, jan 2004.

[13] Karl Gerlach, "Outlier resistant adaptive matched filtering," *IEEE Transactions on Aerospace and Electronic Systems*, vol. 38, no. 3, pp. 885–901, jul 2002.

[14] Christopher M. Teixeira, Jameson S. Bergin, and Paul M. Techau, "Adaptive thresholding of the GIP statistic to remove ground target returns from the training data for STAP applications," in *Adaptive Sensor Array Processing Workshop*, 2004.

[15] Jonathan Bechter ; Fabian Roos ; Mahfuzur Rahman ; Christian Waldschmidt, "Automotive radar interference mitigation using a sparse sampling approach," in *European Radar Conference (EURAD)*, 2017, pp. 90–93.

[16] Muralidhar Rangaswamy, James H. Michels, and Braham Himed, "Statistical analysis of the non-homogenity detector for STAP applications," *Digital Signal Processing*, vol. 14, no. 3, pp. 253–267, may 2004.

[17] James Ward, "Space-time adaptive processing for airborne radar," Tech. Rep. 1015, MIT Lincoln Laboratory, 1994.

[18] Jian Li and Petre Stoica, Eds., *Robust Adaptive Beamforming*, chapter 8. Diagonal loading for finite sample size beamforming an asymptotic approach, John Wiley and Sons, 2005.

[19] Harry L. Van Trees, *Optimum Array Processing*, Detection, Estimation and Modulation Theory. "John Wiley and Sons, Inc.", 2002.

[20] Jian Li, Petre Stoica, and Zhisong Wang, "On robust capon beamforming and diagonal loading," *IEEE Transactions on Signal Processing*, vol. 51, no. 7, pp. 1702–1715, jul 2003.

[21] Johan Degerman, "Statistical analysis of multi-channel detection using data from airborne aesa radar," in *Acoustics, Speech, and Signal Processing, ICASSP IEEE*, 2011.